Available online at www.iseec2012.com

I-SEEC 2012

Proceeding - Science and Engineering (2013) 457–464

Proceeding
Science and Engineering

www.iseec2012.com

Science and Engineering Symposium
4th International Science, Social Science, Engineering and Energy Conference 2012

Highly THz Frequency Carrier Generated by a PANDA for Ad Hoc Networks for Ubiquitous Computer Use

S. Songmuang[a,*], S.Punthawanunt[a], N. Thammawongsa[b], P.P. Yupapin[c]

[a]*Faculty of Science and Technology,Kasem Bundit University, Bangkok 10250, Thailand*
[b]*Hybrid Computing Research Laboratory, Faculty of Engineering;*
[c]*Nanoscale Science and Engineering Research Alliance (N'SERA), Advanced Research Center for Photonics, Faculty of Science, King Mongkut's Institute of Technology, Ladkrabang, Bangkok 10520, Thailand*

Abstract

This paper proposed the THz frequency generation by using a novel microring resonator called "PANDA ring" with Gold nano-antenna coupling to active plasmonic devices at THz for network applications. The dense wavelength division multiplexing (DWDM) can be generated and obtained by using a Dark-Bright soliton conversion control propagating within a modified PANDA ring resonator and an add-drop filter systems. The proposed system results demonstrated Dark-Bright soliton conversion control and the frequency obtained in THz frequency band. Finally, this area of frequency provides a reliable frequency band for a new generation ubiquitous computer network use.

Selection and/or peer-review under responsibility of Faculty of Science and Technology, Kasem Bundit University, Bangkok.

Keywords: Ad-hoc network, an add/drop filter, DWDM, PANDA Ring, THz technology, nano-antenna, Ubiquitous Computer;

1. Introduction

Recently, the amount of data transmission is increasing with a rising demand of the high-bandwidth carrier operating in the high frequency. Various high frequency researches have been used in different fields such as, imaging diagnosis, [1] physics, [2] magnetic, [3] neuroscience, [4] acoustics, [5] ultrasonic, [6] electronics, [7] etc. The THz signals generation has become an interesting subject with the availability of a highly investigated and several solutions. The important factors for THz-wave generation are High nonlinearity and Good transparency at THz frequency region that it was produced by a nonlinear crystal. [8] The high frequency electromagnetic sensor using Magnetic Garnet was shown in [3] which far-infrared magnetic resonances were measured at the high frequencies up to 315 GHz in pulsed high magnetic field. Moreover, there is an examination of the high-frequency capability of carbon nanotube by using CNFETs (Carbon nanotube field effect transistors). The reduction of metallic tubes number in CNFETs created from multiple nanotubes has

* Corresponding author.*E-mail address:* st.songmuang@gmail.com.

allowed the measured frequency to be increased to 30 GHz. [7] Then, highly coherent THz wave generation using a dual frequency Brillouin fiber laser and a 1.55 μm photomixer was demonstrated [9]. This method is composed of a uni-travelling carrier photodiode integrated with an antenna that is observed a ~ 1 kHz linewidth emission at 316 GHz, with a signal to noise ratio > 65 dB. For spectroscopic applications, an optical monochromatic sub-terahertz signal generation technique using an optical comb signal, arrayed waveguide gratings (AWGs), and a uni-traveling carrier photodiode (UTC-PD) offers broadband tunability, fast frequency control, very narrow linewidth, fine tuning resolution, external instruments frequency locking, and reliable operation with frequency tuning in the range between 100 GHz and up to 1 THz. [10] In addition, an optical signal generation technique produces the high THz frequency and large bandwidth which play the important role in the next generation communication.

In 1980s [9], EM wave at 1mm-100 μm band was called THz gap because of the low energy, high efficiency, stable, and low cost. The THz source was found that there were three key parameters which are tunability, available power and associated phase noise. The THz frequency generation technique can be applied in optical and wireless networks that have reported a new all-optical VPN (Virtual Private Network) scheme operating at 10 Gbit/s in 16 QAM (Quadrature amplitude modulation) OFDMA-PON (Orthogonal Frequency Division Multiple Access-based Passive Optical Network). All-optical VPN and all-optical inter-ONU (Optical Network Units) communications enabled at the same time, [11] increased long distance and high-bandwidth communications. Currently, the new approach to carry peer-to-peer communications in the integrated optical wireless access networks called FiWi networks was presented. The interference in wireless subnetwork can be sustained and its network throughput can be improved. [12] Furthermore, optical and wireless networks are effective and very useful for wireless mobile, Mobile Ad Hoc Network (MANET), a various mobile hosts forming a temporary network without any centralized administration or established infrastructure. These was presented in the enhancing throughput efficiency of ad hoc wireless networks using cognitive radio technique for self-aware and self-organized ad hoc wireless networks. [13]

Most of the work on optical frequencies generation has focused on plasmonics mechanism. [14-17] The reason for this focus lies on the strength of coupling between the radiation and the free electrons, which is determined by the permittivity of the conductor. This coupling is optimum—the confinement of the surface plasmon polaritons (SPPs) to the surface is maximum when the absolute value of the permittivity is small, at optical frequencies for noble metals such as gold and silver. Metals at THz frequencies have very large permittivities, which lead to a weak confinement of SPPs to the surface. As we will see next, semiconductors have a much lower permittivity than metals at THz frequencies, mainly due to their much lower free carrier concentration. This permittivity allows for a strong coupling of the THz field to free charges at the interface and a good confinement of the surface mode to the interface.

This paper demonstrated the THz frequency generation by using a novel microring resonator called “PANDA ring” with Gold nano-antenna coupling to active plasmonic devices at THz for network applications. The dense wavelength division multiplexing (DWDM) can be generated and obtained by using a Dark-Bright soliton conversion control propagating within a modified PANDA ring resonator and an add-drop filter systems. The proposed system results demonstrated Dark-Bright soliton conversion control and the frequency obtained in THz frequency band. Finally, this area of frequency provides a reliable frequency band for a new generation ubiquitous computer network use.

2. THz frequency carrier generation

2.1 PANDA ring resonator

In this study, a modified add-drop filter called “PANDA” ring resonator which contains nano and micro ring being integrated together is proposed. The system achieves dark-bright soliton conversion process, which produces the orthogonal set of dark and bright soliton pair and can be decomposed into left and right circularly polarized waves. The relative phase of the two output light signals is $\pi/2$ after coupling into the optical coupler. In addition, the signals produced from the throughput port and drop port has a π phase change from the original

input signal. The concept of orthogonal soliton spins can be assigned as the optical dipoles. The proposed system is introduced into the modified add-drop optical filter system as shown in Fig.1.

Input and Add signals in the form of dark and bright optical solitons are governed by the equations (1) and (2) respectively [18].

$$E_{in1}(t) = A\tanh\left[\frac{T}{T_0}\right]\exp \mathrm{M}, \qquad (1)$$

$$E_{add}(t) = A\,\mathrm{sech}\left[\frac{T}{T_0}\right]\exp \mathrm{M}, \qquad (2)$$

Where $\mathrm{M} = \left[\left(\frac{x}{2L_D}\right) - i\varnothing(t)\right]$,

which A and x are the optical field amplitude and propagation distance, respectively. The random phase term related to the temporal coherence function of the input light as follow.

$$\phi(t) = \phi_0 + \phi_{NL} = \phi_0 + \frac{2\pi n_2 L}{A_{eff}\lambda}\left|E_0(t)\right|^2, \qquad (3)$$

The linear phase shift is ϕ_0, ϕ_{NL} is the nonlinear phase shift; n_2 is the nonlinear refractive index of ***InGaAsP/InP*** waveguide. The effective mode core area of the device is given by A_{eff}, $L = 2\pi R_{ad}$; R_{ad} is the radius of device; λ is the input wavelength light field, and $E_0(t)$ is the circulated field within nanoring coupled to the right and left add-drop optical filter system as shown in figure 1. T is a soliton pulse propagation time in a frame moving at the group velocity; T_0 is a soliton pulse propagation time at initial input; $T=t-\beta_1*x$, where β_1 and β_2 are the coefficients of the linear and second-order terms of Taylor expansion of the propagation constant. $L_D = T_0^2/|\beta_2|$ is the dispersion length of the soliton pulse, where t is the soliton phase shift time, and the frequency shift of the soliton is ω_0. This solution describes a pulse that keeps its temporal width invariance as it propagates, and thus is called a temporal soliton. The refractive index (n) of light propagates within the medium is given by

$$n = n_0 + n_2 I = n_0 + \frac{n_2}{A_{eff}}\,P\,, \qquad (4)$$

where n_0 and n_2 are the linear and nonlinear refractive indexes. I and P are the optical intensity and optical power. A_{eff} is the effective mode core area of system. For the MRR and NRR, the effective mode core areas range from 0.05 to 0.10 μm^2 [19], [20].

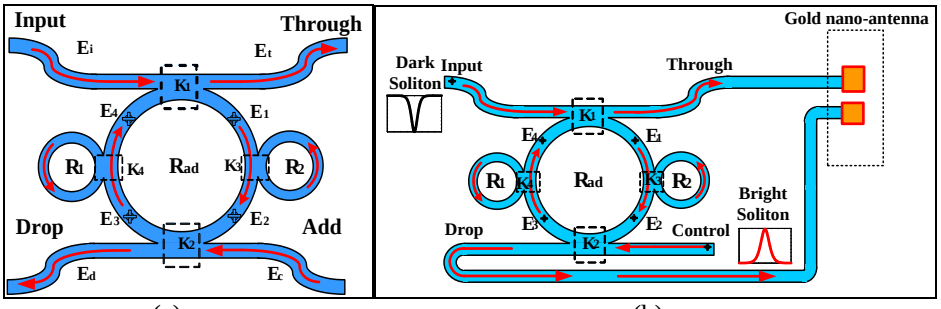

Fig.1. Schematic of multi-optical spins generated by soliton pulse in a PANDA ring resonator
a) traditional PANDA ring resonator b) Gold Nano-antenna coupled PANDA ring resonator for THz generation

In Fig.1, the PANDA ring resonator generates orthogonal set of dark and bright soliton pair. The add-drop optical filter device is used to radiate transverse magnetic field by spin polarization. The output field, E_T and E_1

consists of the transmitted and circulated components within add-drop optical multiplexing system, which provides the driving force to photon/molecule/atom. Analytically, for the light pulse to pass through the coupler of the PANDA multiplexing system [21], the transmitted and circulated components can be written as

$$E_T = Y_1\left[X_1 E_{in1} + \sqrt{\kappa_1} E_4 \right], \quad (5)$$

$$E_1 = Y_1\left[X_1 E_4 + \sqrt{\kappa_1} E_{in1} \right], \quad (6)$$

$$E_2 = E_{R2} E_1 exp\left[-\frac{a}{2}\frac{L}{2} - j\kappa_n \frac{L}{2} \right], \quad (7)$$

Where $Y_1 = \sqrt{1-\gamma_1}$, $X_1 = \sqrt{1-\kappa_1}$

For the second coupler of the add-drop optical multiplexing system

$$E_D = Y_2\left[X_2 E_{i2} + \sqrt{\kappa_2} E_2 \right], \quad (8)$$

$$E_3 = Y_2\left[X_2 E_2 + \sqrt{\kappa_2} E_{i2} \right], \quad (9)$$

$$E_4 = E_{R1} E_3 exp - \frac{\infty}{2}\frac{L}{2} - \mathrm{j}\kappa_n \frac{L}{2}, \quad (10)$$

Where $Y_2 = \sqrt{1-\gamma_2}$, $X_2 = \sqrt{1-\kappa_2}$

Where κ_1 and κ_2 is the intensity coupling coefficient; γ_1 and γ_2 is the fractional coupler intensity loss; α is the attenuation coefficient; κ_n = 2π/λ is the wave propagation number; λ is the input wavelength light field, and L=2πR$_{ad}$R$_{ad}$ is the radius of add-drop device. For the circulated light fields, E_{R1} and E_{R2} are the light field circulated components of the nanoring radii, R_1 and R_2 which coupled into the left and right sides of the add-drop optical multiplexing system, respectively. The light field transmitted and circulated components in the right nanoring, E_{R1} and E_{R2}, are given by

$$E_{R1} = E_3\left\{ \frac{\sqrt{Y_4 X_4} - Y_4 \exp -\frac{a}{2}L_1 - j\kappa_n L_1}{1 - \sqrt{Y_4 X_4}\exp -\frac{a}{2}L_1 - j\kappa_n L_1} \right\}, \quad (11)$$

$$E_{R2} = E_1\left\{ \frac{\sqrt{Y_3 X_3} - Y_3 \exp -\frac{a}{2}L_2 - j\kappa_n L_2}{1 - \sqrt{Y_3 X_3}\exp -\frac{a}{2}L_2 - j\kappa_n L_2} \right\}, \quad (12)$$

Where $Y_3 = (1-\gamma_3), Y_4 = (1-\gamma_4)$, $X_3 = (1-\kappa_3)$; κ_3 and κ_4 are the intensity coupling coefficient, γ_3 and γ_4 is the fractional coupler intensity loss; α is the attenuation coefficient; $\kappa_n = 2\pi/\lambda$ is the wave propagation number; λ is the input wavelength light field, and $L_1 = 2\pi R_1$, R_1 is the radius of left nanoring.

The output optical field of the through port (E_T) and the drop port (E_D) are expressed by

$$E_T = x_1 y_1 E_{in1} + \left(j x_1 x_2 y_2 \sqrt{\kappa_1} E_{R2} E_{R1} E_1 - x_1 x_2 \sqrt{\kappa_1 \kappa_2} E_{R1} E_{add} \right) \exp TP, \quad (13)$$

$$E_D = x_2 y_2 E_{add} + j x_2 \sqrt{\kappa_2} E_{R2} E_1 \exp TP, \quad (14)$$

Where $TP = -\frac{a}{4}\frac{L}{4} j\kappa_n \frac{L}{4}$,

2.2 Gold Nano-antenna plasmonic devices at THz

The characteristic lengths of surface plasmon polaritons, namely the SPPs wavelength (λ spp), propagation length (Lspp) and confinement to the surface (Lz) can be derived from the SPPs complex wave number, which is given by

$$L_{spp} = \sqrt{\frac{1}{2\Im(k_{spp})}}. \quad (15)$$

$$\kappa_{spp} = \frac{\omega}{c}\sqrt{\frac{\varepsilon_c \varepsilon_d}{\varepsilon_c + \varepsilon_d}}, \quad (16)$$

where ω is the angular frequency, c the speed of light in vacuum, and ω_c and ω_d are the relative permittivity of the conductor and the dielectric respectively. For simplicity, we will consider vacuum as the dielectric with ε_d = 1. The relative permittivity of the conductor is a complex quantity, $\varepsilon_c = \Re(\varepsilon_c) + i\Im(\varepsilon_c)$, which can be approximated by a Drude model for free charge carriers [22]

$$\varepsilon_c = \varepsilon_\infty \left(1 - \frac{\omega_P^2}{\omega^2 + i\gamma\omega}\right), \quad (17)$$

where ε_d is the high-frequency permittivity; γ is the average collision rate of the charge carriers and $\omega_P = \sqrt{Ne^2 / \varepsilon_\infty \varepsilon_0 m^*}$ is the plasma frequency. The waveguide charge carrier concentration is given by N, while e is the fundamental charge, ε_0 the vacuum permittivity and m^* the charge effective mass.

3. Results and Discussion

In process, the orthogonal soliton sets can be generated by using the system in PANDA ring resonator. The optical field is fed into the ring resonator system, where R_1 = R_2 = 2.5μm, R_{ad} = 30μm by using a microring, R_{Th}= R_{Ct}= 20μm. To form the initial spin states, the field is induced by an Au coupled on InGaAsP waveguides for THz generation states. In this simulation, the coupling coefficient ratios κ_1:κ_2 are 50:50, 90:10, 10:90 and the ring radii R_{ad} = 30μm, A_{eff} = 0.25μm^2, n_{eff} = 3.14 (for InGaAsP/InP), α= 0.1dB/mm, γ= 0.01, λ_0= 1.55 μm is shown in Figure 1. The THz was generated by a dark-soliton pump based-on through port and drop port microring resonator gold coated at center wavelength 1.55μm as shown in Fig.4.

For gold as a function of frequency, the free carrier concentration of gold is $N \approx 6\times10^{22} cm^{-3}$ and the plasma frequency is $\omega_P / 2\pi \approx 2\times10^3$ THz [23]. At high frequencies, in the visibility, the real and imaginary components of the permittivity of gold have a small value. As the frequency decreases, the permittivity increases due to the ω^{-2} dependence in Eq. (18). At THz frequencies the permittivity has large absolute values in fig.2. Note that in spite of the large value of the imaginary component of the permittivity of gold, the surface wave can propagate a long distance of several meters along the surface. This long propagation length is a direct consequence of the weak coupling of the field with the charges and the small penetration of this field in the metal. In this proposed work, the power radiation and field enhancement are illustrated in Figure 3, which shows that the power transmission from the antenna and normalized filed enhancement are compared by varying the coupling effect between the through port and Drop port SPPs. This design results present the optical THz generation method, in which the radio frequency can be radiated by using the simple nano-antenna model.

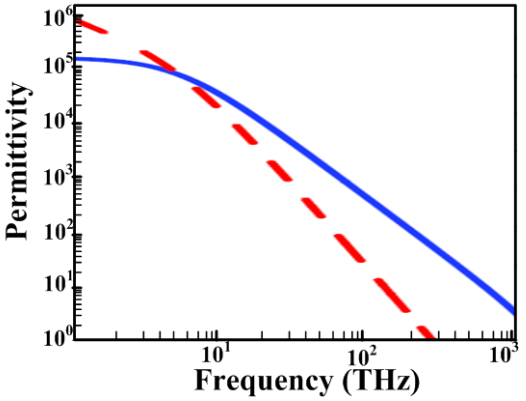

Fig. 2. Complex permittivity ε_c of gold as a function of frequency, the solid lines represent $-\Re(\varepsilon_c)$, while the dashed line is $\Im(\varepsilon_c)$

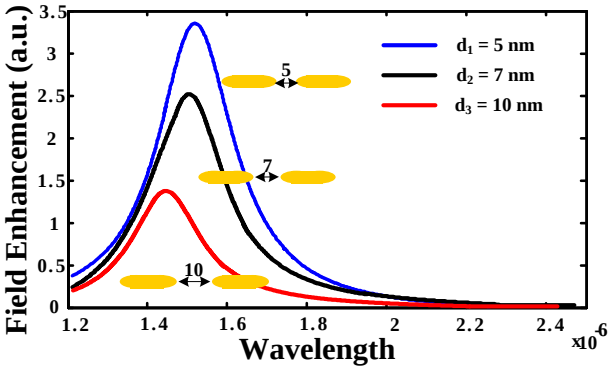

Fig. 3. Nano-antenna field enhancement [24]

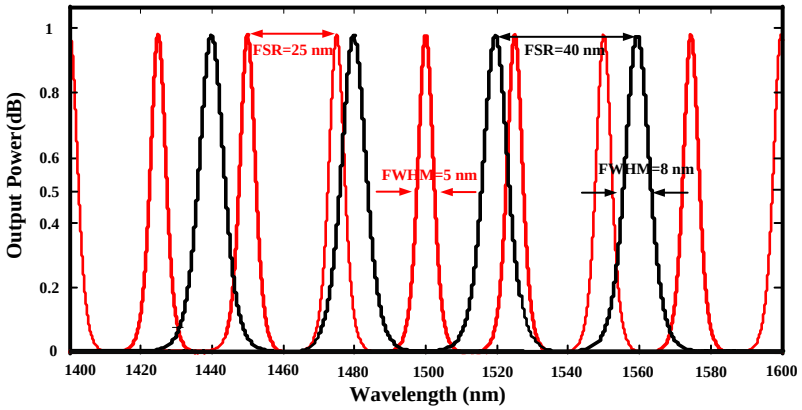

Fig. 4. THz Generation by using PANDA ring resonator with Gold nano-antenna coupling to active the narrower wavelength (in red) than wavelength (in black) which is none coupling with Gold nano-antenna. Therefore, the narrow/short wavelength (in red, FSR = nm) will be produced the highly THz frequency and large bandwidth that increased long distance and high-bandwidth communications

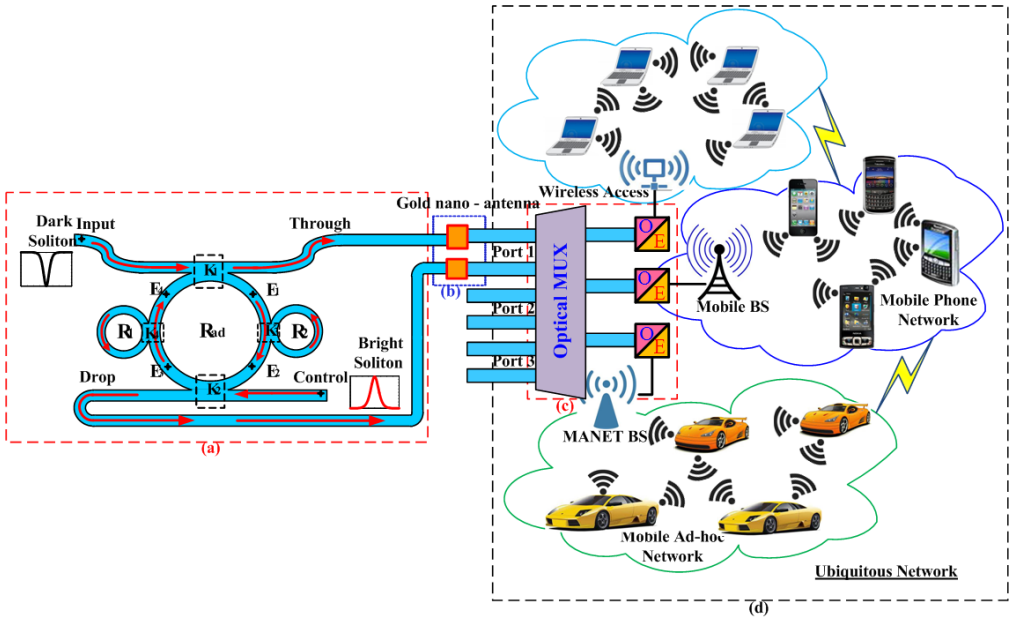

Fig. 5. Integrated system design for ubiquitous network

For the figure shown, (a) a Dark-Bright soliton conversion control propagating within a modified PANDA ring resonator and an add-drop filter systems generated the THz frequency. (b) The THz frequency generation by using Gold nano-antenna coupling to active plasmonic devices at THz which is the plasmonics mechanism can produce the highly THz frequency and large bandwidth that increased long distance and high-bandwidth communications. (c) The power transmission from the antenna will fluctuate the coupling effects by using the Optical MUX to execute an O/E. (d) Uubiquitous network, which is proposed, is a reliable frequency band that can be applied in various optical and wireless networks such as, wireless access, mobile base station, MANET base station, and etc.

4. Conclusion

In conclusion, our results demonstrate that the THz frequency generation by using PANDA ring resonator with Gold nano-antenna coupling to active plasmonic devices at THz. In case of the permittivity of gold, the surface wave can propagate a long distance of several meters along the surface that can produce narrower wave length than non-coupling by Gold nano-antenna, and highly THz frequency occurs. Therefore, the system results provide a highly frequency and a reliable frequency band for various applications in ubiquitous computer network use.

References

[1] Liset Menendez de la Prida, Andrew J. Trevelyan, "Cellular mechanisms of high frequency oscillations in epilepsy: On the diverse sources of pathological activities," Epilepsy Research, Vol. 97, pp. 308-317, 2011.

[2] Ruediger Groening, Hubert Bensmann, "High frequency controlled capsules with integrated gas producing cells," European Journal of Pharmaceutics and Biopharmaceutics, Vol. 72, pp. 282-284, 2009.

[3] Nobuyasu Adachi, Daisuke Uematsu, Toshitaka Ota, Masanori Takahashi, Kazushi Ishiyama, Katsumi Kawasaki, Hiroyasu Ota, Kenichi Arai, S. Fujisawa, Susumu Okubo, and Hitoshi Ohta, "Far-Infrared Ferromagnetic Resonance of Magnetic Garnet for High Frequency Electromagnetic Sensor," IEEE Transactions on Magnetics, Vol. 46, No. 6, 2010.

[4] Daniel Harnack, WassiliosMeissner, RaikPaulat, HannesHilgenfeld, Wolf-Dieter M¨uller, Christine Winter, Rudolf Morgenstern, Andreas Kupsch, "Continuous high-frequency stimulation in freely moving rats: Development of an implantable microstimulation system," Journal of Neuroscience Methods, Vol. 167, pp. 278-291, 2008.

[5] Toshiyuki Nishiguchi, KimioHamasaki, Kazuho Ono, Masakazu Iwaki, Akio Ando, "Perceptual discrimination of very high frequency components in wide frequency range musical sound," Applied Acoustics, Vol. 70, pp. 921-934, 2009.

[6] Changgeng Liu, Frank Djuth, Xiang Li, Ruimin Chen, Qifa Zhou, K. Kirk Shung, "Micromachined high frequency PMN-PT/epoxy 1–3 composite ultrasonic annular array," Ultrasonics, Vol. 52, pp. 497-502, 2012.

[7] David L. Pulfrey, Li Chen, "Examination of the high-frequency capability of carbon nanotube FETs," Solid-State Electronics, Vol. 52, pp. 1324-1328, 2008.

[8] Kaoru Koketsu, Koji Suizu, Takayuki Shibuya, Toshihiro Tsutsui, and KodoKawase, "Extremely frequency-widened terahertz wave generation using Cherenkov-type radiation," IEEE Conference Publications, Vol. 34, pp. 1-2, 2009.

[9] G. Ducournau, P. Szriftgiser, T. Akalin, A. Beck, D. Bacquet, E. Peytavit and J.F. Lampin, "Dual frequency Brillouin fiber laser and 1.55 µmphotomixer for highly coherent THz wave generation," IEEE Conference Publications, Vol. 36, pp. 1-2, 2011.

[10] Ho-Jin Song, Naofumi Shimizu, TomofumiFuruta, Koji Suizu, Hiroshi Ito, and TadaoNagatsuma, "Broadband-Frequency-Tunable Sub-Terahertz Wave Generation Using an Optical Comb, AWGs, Optical Switches, and a Uni-Traveling Carrier Photodiode for Spectroscopic Applications," Journal of Lightwave Technology, Vol. 26, No. 15, 2008.

[11] J. Toulouse, "Optical Nonlinerities in Fibers: Review, Recent Examples, and Systems Applications," Journal of Lightwave Technology, Vol. 23, No. 11, 2005.

[12] ZeyuZheng, Jianping Wang, Jin Wang, "A Study of Network Throughput Gain in Optical-Wireless (FiWi) Networkd Subject to Peer-to-Peer Communications," IEEE Communications Society, 978-1-4244-3435-0, 2009.

[13] Charushila Axay Patel and Sanjay Kumar, "Enhancing Throughput Efficiency of Adhoc Wireless Networks using Cognitive Radio Approach," IEEE Conference Publications, 978-1-4244-9190-2, 2011.

[14] K J Ahn, K G Lee, H W Kihm, M A Seo, A J L Adam,P C M Planken and D S Kim, "Optical and terahertz near-field studies of surfaceplasmons in subwavelength metallic slits," New Journal of Physics, Vol. 10, 105003, 2008.

[15] AlirezaHassani and MaksimSkorobogatiy, "Surface Plasmon Resonance-like integrated sensor at terahertzfrequencies for gaseous analytes," Optics Express, Vol. 16, No. 25, 20207, 2008.

[16] T. H. Isaac, W. L. Barnes, and E. Hendry, "Determining the terahertz optical properties of subwavelength filmsusing semiconductor surface plasmons," Applied Physics Letters, Vol. 93, 241115, 2008.

[17] Shu-Zee A. Lo and Thomas E. Murphy, "Terahertz surface plasmon propagation in nanoporous silicon layers," Applied Physics Letters, Vol. 96, 201104, 2010.

[18] G. Ducournau, P. Szriftgiser, T. Akalin, A. Beck, D. Bacquet, E. Peytavit and J.F. Lampin, "Dual frequency Brillouin fiber laser and 1.55 µmphotomixer for highly coherent THz wave generation," IEEE Conference Publications, 978-1-4577-0509-0, 2011.

[19] KodoKawase, Takayuki Shibuya, Koji Suizu and Shin'ichiro Hayashi, "Novel THz-wave generation technique and applications," IEEE Conference Publications, pp. 1-4, 2010.

[20] Manoj Kumar and Vipin K. Tripathi, "Resonant Terahertz Generation by Optical Mixing of Two Laser Pulses in Rippled Density Plasma," IEEE Journal of Quantum Electronics, Vol. 48, No. 8, 2012.

[21] P.knobloch, C. Schildknecht, T. Kleine-Ostmann, M. Koch, S. Hoffmann, M. Hofmann, E. Rehberg and K. Pierz, "Medical THz imaging: An investigation of histo-pathological samples," Physics in Medicine and Biology, 47(21): pp. 3875-3884, 2002.

[22] M. van Exter and D. Grischkowsky, "Optical and Electronic properties of doped silicon from 0.1 to 2 THz," Appl. Phys. Lett., Vol. 56, pp. 1694-1696, Apr. 1990.

[23] M.A. Ordal, L.L. Long, R.J. Bell, R.R. Bell, R.W. Alexander Jr, and C.A. Ward, "Optical properties of the metals Al, Co, Cu, Au, Fe, Pb, Ni, Pd, Pt, Ag, Ti, and W in the infrared and far infrared," Appl. Opt., Vol. 22, pp. 1099-1119, Apr. 1983.

[24] N. Thammawongsa, S. Mitatha, P.P. Yupapin, "An optical nano-antenna system design for radio therapeutic use," Progress In Electromagnetics Research Letters, Vol. 31, 75-87, 2012.